

## A Leak Free Phase Change Materials with Enhanced Thermal Buffering Properties by TiO<sub>2</sub>/Biochar

Dessy Ariyanti<sup>1,\*</sup>, Khoirul Huda<sup>1</sup>, Muhammad Bayu Samudra<sup>1</sup>, Dina Lesdantian<sup>1</sup>, Erwan Adi Saputra<sup>2</sup>, Fazlena Hamzah<sup>3</sup>

<sup>1</sup>Department of Chemical Engineering, Faculty of Engineering, Universitas Diponegoro  
Jl. Prof. Soedarto, SH, Tembalang, Semarang

<sup>2</sup>Department of Chemical Engineering, Faculty of Industrial Technology, Universitas Pembangunan Nasional  
“Veteran” Jawa Timur

Jl. Raya Rungkut Madya, Gunung Anyar, Surabaya

<sup>3</sup>Faculty of Chemical Engineering, Universiti Teknologi MARA  
Jl. Ilmu 1/1, Shah Alam, Selangor, Malaysia

\* Corresponding author: [j.reaktor@che.undip.ac.id](mailto:j.reaktor@che.undip.ac.id)

(Received: 18 March 2024; Published: 8 May 2024)

### Abstract

*A leak free organic phase change material of palmitic acid with enhanced thermal buffering properties was synthesized by simple chemical TiO<sub>2</sub>/biochar encapsulation process. By utilizing the optimum amount of TiO<sub>2</sub> as an encapsulation agent the minimalization of leakage phenomena during the phase change process can be achieved with the value 20-25% of weight loss. Furthermore, the additional sugar cane bagasse-based biochar that was introduced to the encapsulation system acts as a support matrix that enhances further the leakage properties into free leak category with the percentage of weight lost 1.1-1.4 %. Moreover, the introduction of sugar cane bagasse-based biochar in the encapsulation system of the palmitic acid PCM can improve the thermal buffering properties by keeping a package box temperature in the range of 2-8°C for more than 20 h by means small increment of temperature 0.72°C/h.*

**Keywords:** PCM, encapsulation, palmitic acid, thermal buffering, leakage

**How to Cite This Article:** Ariyanti, D, Huda, K, Samudra, M.B, Lesdantina, D, Saputra, E.A, and Hamzah, F. (2024), A Leak Free Phase Change Materials with Enhanced Thermal Buffering Properties by TiO<sub>2</sub>/Biochar Encapsulation, Reaktor, 23 (3), 116 - 126, <https://doi.org/10.14710/reaktor.23.3.116-126>

### INTRODUCTION

Phase change material (PCM) is a material that has capability in absorbing and releasing large amounts of energy (energy storage and emission) at its phase transition that occur over a specific temperature

range (Singh et al., 2008; Yang et al., 2019) which can be useful for heating or cooling equipment. PCM as emission storage can be used as thermal buffering support for fruits and vegetables storage system as it has thermal stability and large latent heat storage

compared to other materials. PCM can be categorized as organic and inorganic. Organic PCM such as paraffins, lipids and hydrocarbon are preferable as it is chemically stable and non-reactive in comparison with inorganic PCM. While inorganic PCM have high conductivity in comparison with organic PCM such as fatty acids.

Fatty acids are considered as sustainable PCM as its source came from renewable sources. Fatty acids such as palmitic acid ( $C_{16}H_{32}O_2$ ) can be an excellent PCM for energy storage as its excellent thermodynamic and kinetic characteristics. Palmitic acid is chemically stable, high latent heat, and a low degree of supercooling. However, palmitic acid has several disadvantages, such as low thermal conductivity, and frequent leakage during phase changes, thus limits the use of palmitic acid as PCM (Wan et al., 2019a).

Various studies have been carried out to improve thermal, physical, and energy storage capacity of organic PCM. One of them is the encapsulation method. PCM encapsulation can increase thermal conductivity, thermal reliability, and control volume changes during phase changes (Alva et al., 2017). Research conducted by (Parameshwaran et al., 2013) with ester encapsulation using nano-silver successfully increased the thermal conductivity and reduced the degree of supercooling. However, nano-silver is not preferable as it is not environmentally friendly, toxic, and expensive. Subsequent research was conducted by (Harikrishnan et al., 2017) by encapsulating myristic acid using  $SiO_2$ . However, these studies have not succeeded in increasing PCM's heat capacity. Further research was conducted by (Zhu et al., 2018) with PCM nanoencapsulation using  $SiO_2$ -based materials, which succeeded in reducing latent heat and increasing thermal conductivity. Still, leakage occurred, and the degree of supercooling did not change significantly. Meanwhile, study conducted by Wan et al, by the addition of supporting matrix such as biochar from pinecone can prevent leakage of the palmitic acid PCM as well as improve its thermal conductivity (Wan et al., 2019c).

In this paper the investigation on the effectiveness of encapsulation of palmitic acid PCM with  $TiO_2$  and biochar was reported with the response of its thermal properties as well as leakage phenomena to support the palmitic acid application as PCM for cooling storage box.

## MATERIALS AND METHODS

### Materials

Palmitic acid as PCM based materials, sodium dodecyl sulfate (SDS) as emulsifier, ethanol, and ammonia solution 25% were from Merck, while another chemical such as tetra n-butyl titanate (TNBT) 97% as a precursor for  $TiO_2$  was purchased from Shandong Zhi Shang Chemical Co., Ltd. All chemicals were used without pretreatment.

### Preparation of Biochar

Raw material for biochar synthetization were sugarcane bagasse purchased from the local store in Semarang, Indonesia. Biochar preparation refers to (L. Li et al., 2017) with some modifications. Bagasse firstly dried at  $90^\circ C$  for 3 hours to remove the remaining water content and then mashed into powder. Powder form sugarcane bagasse then transferred into furnace for pyrolysis at  $600^\circ C$  for 2 hours, cooled down to room temperature and then transferred to High Energy Milling (HEM) for final stage biochar production. Biochar then used for further encapsulation process.

### Palmitic Acid Encapsulation as PCM

The palmitic acid encapsulation method refers to the experiment conducted by (Cao et al., 2014). Firstly, 20 g palmitic acid was added to 300 mL DI water and mixed thoroughly followed by the addition of 3 g of sodium dodecyl sulfate (SDS) emulsifier to form an O/W emulsion. The mixture then stirred continuously for 40 minutes at a speed of 1000 rpm all components homogeneously dispersed. The pH value was adjusted in the range 2-3 using HCl. Meanwhile, the encapsulating agent was prepared by dissolving TNBT (10, 15, 20 g) and biochar into 100 mL of ethanol in a ratio (1: 0.00; 1: 0.05; and 1: 0.10). The solution was then added dropwise to the palmitic acid emulsion along with controlled stirring at 800 rpm and operating temperature at  $75^\circ C$  in a water bath for 60 minutes. The mixture was allowed to be cooled down to room temperature and then washed using distilled water and ethanol several times consecutively. The materials then dried at  $45^\circ C$  for 24 hours in a vacuum oven.

### Characterization

Encapsulated PCM were characterized by X-ray powder diffraction (XRD) to determine the crystal phase and its crystallinity. Meanwhile, Fourier-transform infrared (FTIR) spectroscopy analysis were conducted to determine the chemical compositions and the present of palmitic acid in the encapsulated PCM. Scanning electron microscopy (SEM) were performed to investigate the surface morphologies and microstructures of the sample. The phase-change properties and thermal performance of the encapsulated PCM were characterized by differential scanning calorimetry (DSC) using a DSC-60 Plus in nitrogen atmosphere at constant heating with scanning rate of  $10^\circ C/min$ .

### Leakage Test

Leakage test was carried out by heating 1.0 g an encapsulated PCM sample in the oven at  $75^\circ C$  for 15 minutes. The initial sample weight ( $W_0$ ) and the after-test sample weight ( $W_t$ ) were measured and used to calculate the % weight lost (% Wt loss) with the equation 1.

$$\%Wt\ Loss = \frac{|W_t - W_0|}{W_0} \times 100\% \quad (1)$$

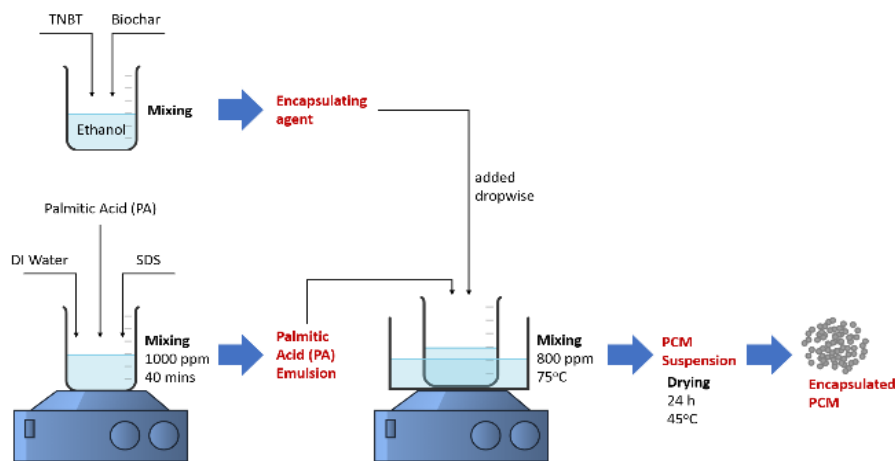


Figure 1. Schematic of PCM encapsulation process

### Thermal Properties Analysis

The performance of encapsulated PCM in maintaining the temperature was tested with the arrangement of several square sample packs filled with encapsulated PCM inside the packaging box to store vegetables as Figure 2. The encapsulated PCM was put into six packs of 500 mL, arranged in a packaging box measuring 19 cm x 14.5 cm x 24 cm with a thickness of 2 cm. Packaging Box is equipped with a data logger thermometer to observe temperature changes inside the box every 10 minutes interval.

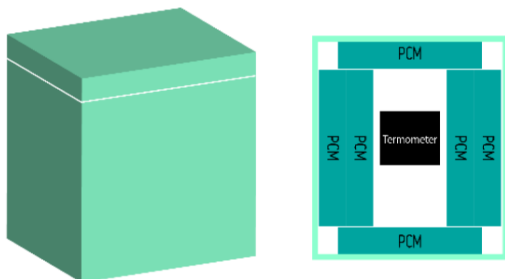
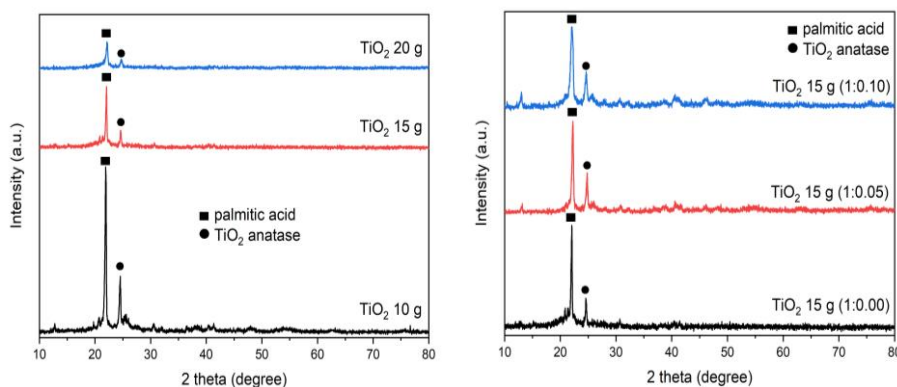


Figure 2. Packaging box for PCM performance analysis

### RESULTS AND DISCUSSION

#### XRD Pattern Analysis of Encapsulated PCM

Fig. 3 shows the XRD patterns of encapsulated PCM at different  $\text{TiO}_2$  addition (a) and with 15 g  $\text{TiO}_2$  addition at variation of biochar ratio (w/w) (b). There are two main peaks series observed in the XRD pattern of all encapsulated PCM. The peaks at two theta  $25^\circ$ ,  $38^\circ$ , and  $48^\circ$  confirms the presence of  $\text{TiO}_2$  anatase phase (JCPDS card 78-2486) (Ariyanti et al., 2018) and peaks at two thetas  $22^\circ$  and  $30^\circ$  confirms the presence of palmitic acid (Sharma et al., 2016a). The main difference observed is the intensity of the peaks. The XRD pattern intensity of encapsulated PCM was decreased by the addition of  $\text{TiO}_2$  as encapsulating agent proving the encapsulation process were successfully performed at the surface of palmitic acid. The same tendency also detected in the addition of biochar ratio (w/w) even though the decreasing of the XRD pattern intensity is not as extreme as in the variation of  $\text{TiO}_2$  alone. The observation on the XRD pattern also indicates that the encapsulation process of PCM using  $\text{TiO}_2$  and  $\text{TiO}_2$ /biochar did not affect the crystal structures of the PCM in this case palmitic acid.

Figure 3. XRD pattern of encapsulated PCM (a) at different  $\text{TiO}_2$  addition; (b) with 15 g  $\text{TiO}_2$  addition at variation of biochar ratio (w/w)

Similar result also reported that the encapsulation of nano-enhanced organic phase change material using  $\text{TiO}_2$  as encapsulating agent did not change the crystal formation of palmitic acid (Sharma et al., 2016a).

### Thermal Energy Storage Properties Encapsulated PCM

DSC analysis was used to determine the thermal properties of encapsulated PCM. The result of the thermal properties of encapsulated PCM at different  $\text{TiO}_2$  additions is presented in Figure 4 with detail value at Table 1. As the temperature of the PCM increases, the microstructure of the PCM begins to stretch, indicating a change in the solid-solid phase. When the temperature is raised further, the molecules of the PCM absorb latent heat and change their phase from solid to liquid, which is the conversion of the absorbed energy into kinetic energy that goes beyond the intermolecular forces. The latent heat data can calculate the PCM encapsulation ratio with the following equation:

$$\eta = \left(1 - \frac{\Delta H_{m,encap PCM}}{\Delta H_{m,PCM}}\right) \times 100\% \quad (2)$$

It can be observed a decrease in the latent heat of PCM along with the addition of  $\text{TiO}_2$  as an encapsulating agent. The latent heat of palmitic acid recorded at 214.36 kJ/kg, while after encapsulation with  $\text{TiO}_2$  decreased to become 141.39; 102.10; and 85.70 kJ/kg for  $\text{TiO}_2$  addition 10; 15; and 20 g respectively. The decrease of latent heat from PCM is due to changes in physicochemical properties due to the dispersion of  $\text{TiO}_2$  particles encapsulated PCM with changes in the ratio of  $\text{TiO}_2$  (Liu et al., 2017; Sharma et al., 2016b; Tao & He, 2018). The latent heat value of PCM is lower than the latent heat of pure palmitic acid because only palmitic acid absorbs thermal energy from the heating process (Cao et al., 2014).

In reverse with the latent heat, the melting point of encapsulated PCM increases with the increase in the

addition of encapsulating agent ( $\text{TiO}_2$ ). DSC analysis shows that pristine palmitic acid has melting point at 62.21°C, slightly increased after the addition of  $\text{TiO}_2$  as encapsulating agent to become 63.80, 64.50, and 64.64°C respectively. The higher the melting point of a material, the better the thermal resistance of PCM to environmental temperatures, as it represents higher sensible heat. It also indicated that the material could receive more heat before it reaches the phase change point (melting point). The shift of melting point occurred in the encapsulated PCM can be assigned as the effect of additional  $\text{TiO}_2$  as encapsulating agent layered the surface of palmitic acid (Arofi, 2016). In addition, the increase in the melting point of encapsulated PCM was also due to an increase in the crystallinity of the PCM core because of the heterogeneous nucleation of the inner wall of the encapsulating agent. This is related to the increase in thermal transfer efficiency resulting from the formation of an encapsulating agent with high conductivity (X. Zhang et al., 2016).

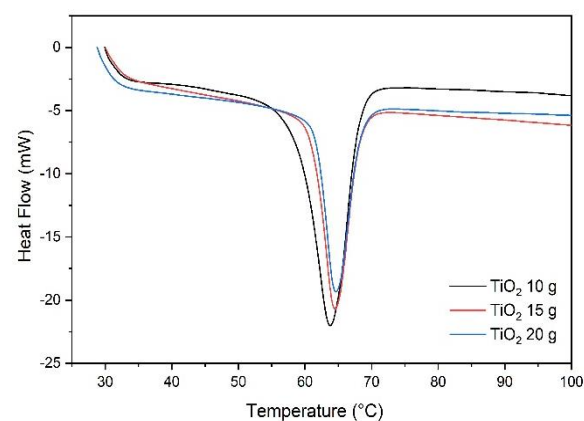


Figure 4. DSC curve of encapsulated PCM at different  $\text{TiO}_2$  addition

Table 1. Latent heat, melting point, and encapsulation ratio of encapsulated PCM at different  $\text{TiO}_2$  addition

No	Variable	Latent Heat (kJ/kg)	Melting Point (°C)	Encapsulation Ratio (%)
1.	Palmitic Acid	214.36	62.21	0
2.	$\text{TiO}_2$ 10 g	141.39	63.80	34.04
3.	$\text{TiO}_2$ 15 g	102.10	64.50	52.37
4.	$\text{TiO}_2$ 20 g	85.70	64.64	60.02

Table 2. Latent heat, melting point, and encapsulation ratio of encapsulated PCM with 15 g  $\text{TiO}_2$  addition at variation of biochar ratio (w/w)

No	Variable	Latent Heat (kJ/kg)	Melting Point (°C)	Encapsulation Ratio (%)
1.	Palmitic Acid	214.36	62.21	0
2.	$\text{TiO}_2$ 15 g (1:0.00)	102.10	64.50	52.37
3.	$\text{TiO}_2$ 15 g (1:0.05)	110.50	62.98	48.54
4.	$\text{TiO}_2$ 15 g (1:0.10)	112.94	65.36	47.31

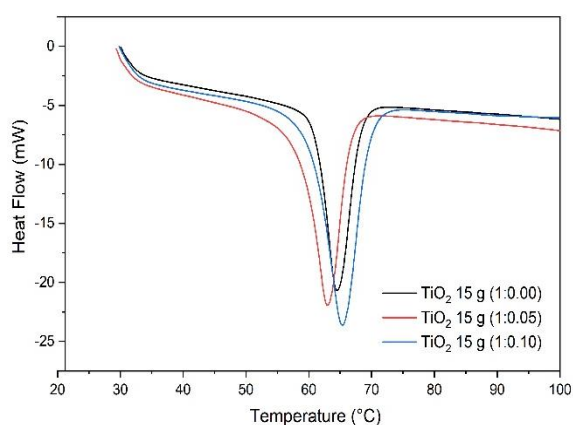


Figure 5. DSC curve of encapsulated PCM 15 g TiO<sub>2</sub> addition at variation of biochar ratio (w/w)

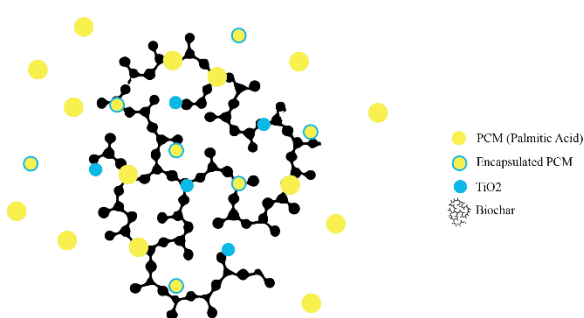


Figure 6. Illustration of TiO<sub>2</sub> and biochar encapsulated PCM

On the other hand, the increase of the PCM encapsulation ratio instigates the lower value of latent heat. This implies the encapsulation material added to the surface of PCM creates a layer that prevent the PCM to act as a latent heat storage. Thus, the layer should be controlled to get the optimum latent heat storage capacity with extensive amount of storage time and other additional properties required.

Based on the latent heat data obtained at different biochar additions, the higher content of biochar brings higher latent heat of encapsulated PCM as illustrated in Figure 5 and Table 2. The presence of biochar in this PCM-TiO<sub>2</sub> encapsulation system creates a new phenomenon that the TiO<sub>2</sub> adsorbed in the pores of biochar (illustrated in Figure 6) resuming low encapsulation ratio and leaves the unencapsulated PCM outside the biochar leads to higher latent heat. The more unencapsulated PCM, the latent heat increases because only palmitic acid absorbs thermal energy from the heating process (Cao et al., 2014). Higher latent heat also represents the smaller number of encapsulated PCMs. In encapsulation using biochar, the interaction between particles occurs through surface tension, capillary forces, and hydrogen bonds between the palmitic acid chain and biochar pores, so that changes occur only physically, while the crystal structure and chemical properties of palmitic acid do not change (Feng et al., 2011; Wan et al., 2019c).

### Effect of Encapsulating Agent on Mechanical Properties of Encapsulated PCM

Leakage is a phenomenon that occurs when PCM undergoes a phase change from solid to liquid, thus limiting the use of PCM (H. Li et al., 2014) for applications and commercialization.

Many approaches have been conducted to minimize the leakage phenomena and so far, the most effective method to prevent PCM leakage into the system is encapsulating PCMs using other supporting materials (Ramakrishnan et al., 2017). Encapsulation is an approach that providing support structure for the palmitic acid as PCM thus inhibit excessive interaction with its surrounding as well as increasing the area of heat transfer, preventing leakage and improve the PCM compatibility with the environment. The encapsulation process involving the incorporation of matrix to the PCM and PCM act as a core. The matrix might be capable of resisting the stress produced due to the volumetric evolution as the PCM changes its phase.

Table 3 and Figure 7 show the leakage test result of encapsulated PCM at different TiO<sub>2</sub> addition. Based on the results, with the increasing concentration of TiO<sub>2</sub> up to 15 gr, the leakage phenomenon can be minimized up to 10%. However, TiO<sub>2</sub> addition more than 15 gr shows more leakage in the encapsulated PCM. This is because additional TiO<sub>2</sub> might produce ticker shell walls that crack easily at high temperatures provide a pathway for palmitic acid to leak to the outer of the shell (Drissi et al., 2020; C. Li et al., 2018).

Table 3. Leakage test result of encapsulated PCM at different TiO<sub>2</sub> addition

No	Variable	% wt loss	Leakage observation
1.	TiO <sub>2</sub> 10 g	32.20%	Positive
2.	TiO <sub>2</sub> 15 g	21.60%	Positive
3.	TiO <sub>2</sub> 20 g	25.40%	Positive

Table 4. Leakage test result of encapsulated PCM at different TiO<sub>2</sub> and biochar ratio

No	Variable	% wt loss	Leakage observation
1.	TiO <sub>2</sub> 15 g (1:0.00)	21.60%	Positive
2.	TiO <sub>2</sub> 15 g (1:0.05)	1.40%	Negative
3.	TiO <sub>2</sub> 15 g (1:0.10)	1.10%	Negative

On the other hand, as illustrated in Table 4 and Figure 8, the addition of biochar with the ratio 1:0.10 (w/w) has successfully prevented the leakage phenomena up to 20%. Biochar is carbon materials that has high surface area, micropore structure, and absorption capacity, which allows palmitic acid as PCM to be evenly adsorbed and dispersed in biochar (Zhou et al., 2020).

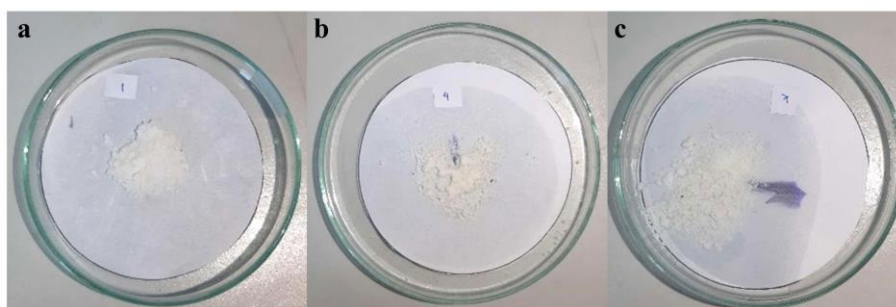


Figure 7. Leakage test visualization of encapsulated PCM (a)  $\text{TiO}_2$  10 g; (b)  $\text{TiO}_2$  15 g; and (c)  $\text{TiO}_2$  20 g addition

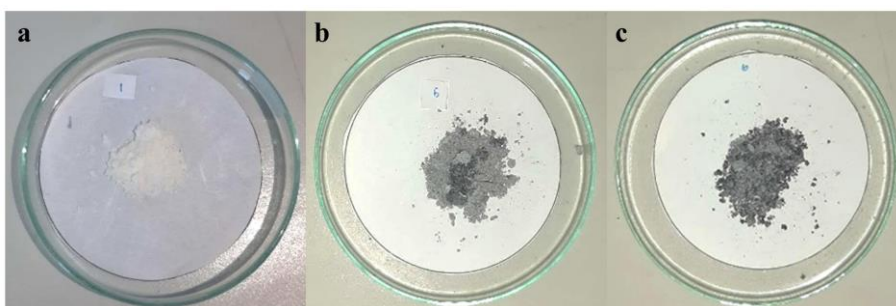


Figure 8. Leakage test visualization of encapsulated PCM (a)  $\text{TiO}_2$  15 g (1:0.00); (b)  $\text{TiO}_2$  15 g (1:0.05); and (c)  $\text{TiO}_2$  15 g (1:0.10)

According to (Wan et al., 2019), the effect of large pore volume and biochar surface area is very beneficial for PCM because it can prevent leakage phenomena during the phase change process.  $\text{TiO}_2$  is a material that can increase thermal stability and conductivity and its inert and non-toxic properties, making  $\text{TiO}_2$  a good encapsulating agent (Cao et al., 2014). Meanwhile, biochar has a high surface area and high absorption capacity, increasing thermal stability, thermal conductivity and preventing leakage (Wan et al., 2019a). Biochar is made by utilizing bagasse waste which contains high carbon and has excellent economic prospects to be developed.

#### Effect of Encapsulating Agent on Thermal Properties of the PCM

The thermal properties of the encapsulated palmitic acid PCM were determined by performing the application test to measure the temperature consistency (thermal buffering properties) over time. The application was conducted in a box packaging with encapsulated palmitic acid PCM pack equipped with a data logger thermometer to observe temperature changes in the box every 10-minute interval. Figures 9 and 10 illustrate the thermal buffering profile of encapsulated PCM at different  $\text{TiO}_2$  addition and variation of biochar ratio (w/w). In the variation of  $\text{TiO}_2$  addition as encapsulated agent, the thermal buffering properties were reduced by the addition of  $\text{TiO}_2$ . The temperature rose  $0.84^\circ\text{C}/\text{h}$ ;  $1.03^\circ\text{C}/\text{h}$ ; and  $1.31^\circ\text{C}/\text{h}$  for  $\text{TiO}_2$  addition 10; 15 and 20 g respectively in the span of 2-8°C. The tendency is due to the latent heat profile from the encapsulated PCM causes the heat storage capacity of the PCM to

decrease (Cao et al., 2014). As mentioned in Table 1 (previous section), the difference in latent heat can be observed according to the concentration of  $\text{TiO}_2$  in the encapsulated PCM. The higher the  $\text{TiO}_2$  concentration in the PCM, the lower the latent heat value of the PCM, which results in a reduced heat storage capacity.

Meanwhile, the addition of biochar as matrix to support the palmitic acid PCM that mixed with the encapsulation agent  $\text{TiO}_2$ , provides good thermal buffering properties. The temperature rose  $1.03^\circ\text{C}/\text{h}$ ;  $0.96^\circ\text{C}/\text{h}$ ; and  $0.72^\circ\text{C}/\text{h}$  for biochar ratio with  $\text{TiO}_2$  0; 0.05 and 0.1 (w/w) respectively in the span of 2-8°C. The greater the biochar content in PCM, the higher the latent heat value which results in an increased heat storage capacity. The greater the palmitic acid concentration in the encapsulated PCM, the higher the latent heat, which results in the PCM being able to absorb and release higher energy.

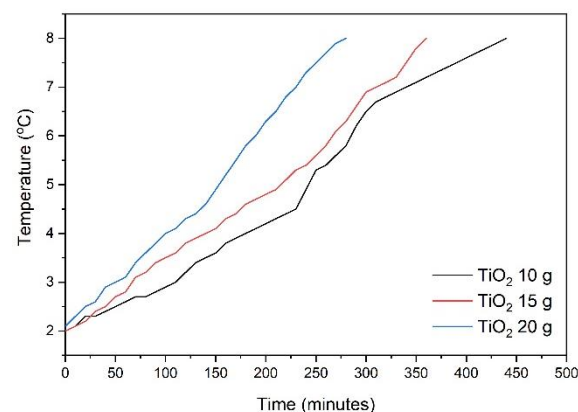


Figure 9. Thermal buffering profile of encapsulated PCM at different  $\text{TiO}_2$  addition

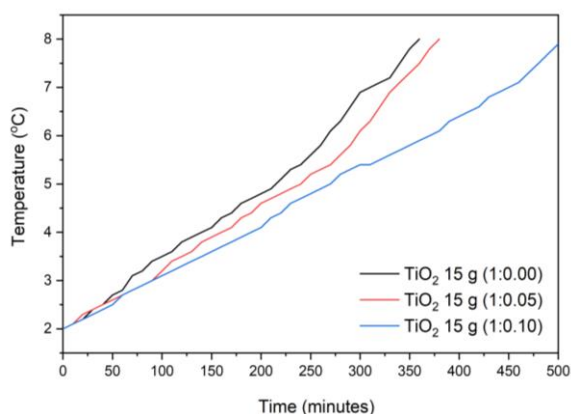


Figure 10. Thermal buffering profile of encapsulated PCM with 15 g of  $\text{TiO}_2$  addition variation of biochar ratio (w/w)

### Morphology and Nanostructures of $\text{TiO}_2$ Encapsulated PCM

The morphology and nanostructures of the  $\text{TiO}_2$  encapsulated PCM were observed by SEM image. The SEM characterization of different biochar addition was carried out with 10,000x and magnification of 20,000x as can be seen in Figure 11. In the SEM image it can be observed that the biochar in the encapsulated palmitic acid PCM system as hypothesis act like matrix that support the encapsulated palmitic acid. It also observed that the encapsulation was successfully formed with spherical shapes with varied size from 300-800 nm. The higher

biochar addition the variation of the encapsulation size becomes more severe. The biochar produced from sugarcane bagasse as suspected has massive pores that interrupted the encapsulation growth thus creating many small nuclei of encapsulated palmitic acid.

From SEM image it also can be observed that the formation of a  $\text{TiO}_2$  shell layer from the TNBT precursor solution can hold the palmitic acid to remain in the capsule during phase changes which can prevent leakage but might reduce the thermal properties (X. Zhang et al., 2016). Meanwhile the addition of biochar large surface area and pore volume, it adheres the PCM to the surface of the biochar thus improve the leak free and thermal properties (Wan et al., 2019a).

### Functional Group Analysis of the Encapsulated PCM

FTIR spectra of encapsulated PCM with different  $\text{TiO}_2$  addition and at various ratios of biochar are shown in **Figure 12**. The band between 400 and 800  $\text{cm}^{-1}$  represents the Ti-O vibrations. The peaks at 2915 and 2848 show the symmetrical stretching vibration of  $-\text{CH}_3$  and  $-\text{CH}_2$  group in palmitic acid. C = O stretching vibration is assigned by a peak seen at 1696  $\text{cm}^{-1}$ . The deformation-vibration of  $-\text{CH}_3$  and  $-\text{CH}_2$  group in palmitic acid represented at the peak of 1462  $\text{cm}^{-1}$ . The peaks 940  $\text{cm}^{-1}$  correspond to the in-plane and out plane bending vibration of the  $-\text{OH}$  group of palmitic acid. The symmetric peaks at 728  $\text{cm}^{-1}$  correspond to the swinging vibration of the  $-\text{OH}$  functional group (Sharma et al., 2016).

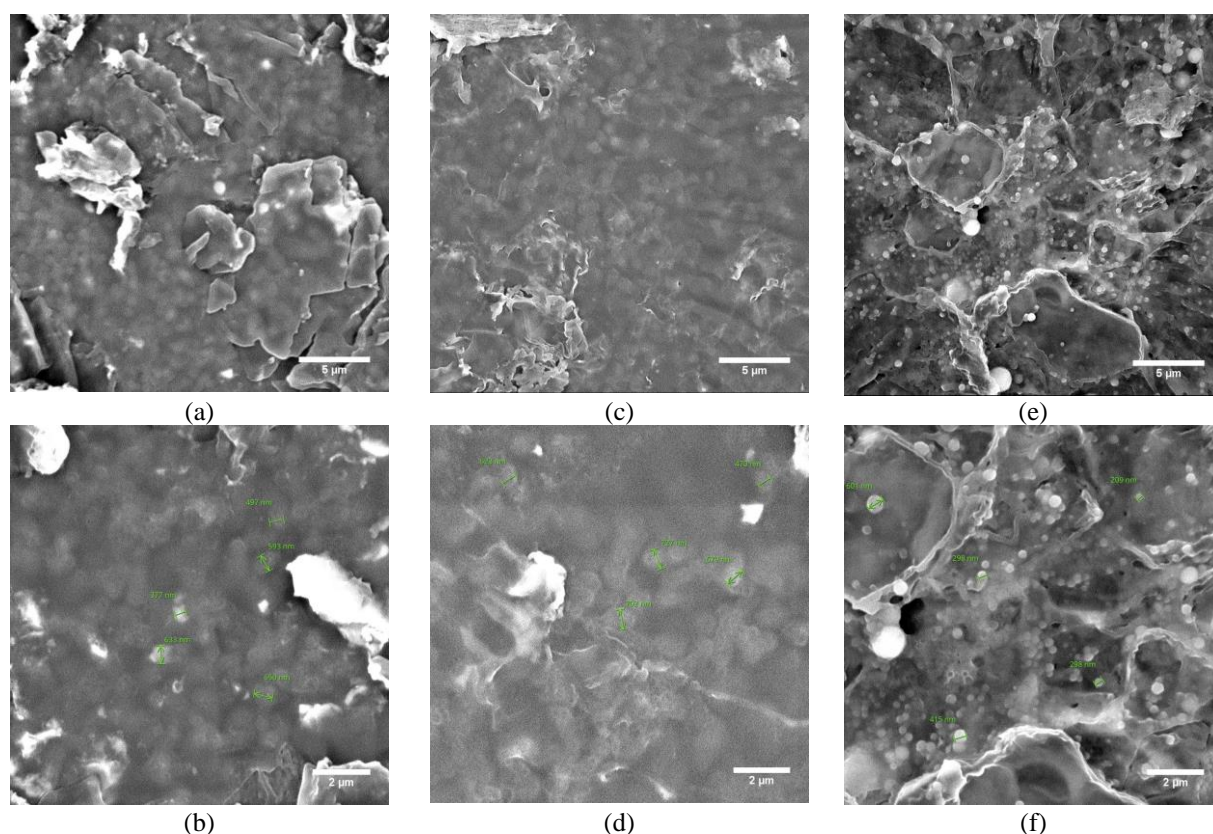


Figure 11. SEM results of encapsulated PCM with 15 g  $\text{TiO}_2$  addition at variation of biochar ratio (w/w) (a-b) 1:0; (c-d) 1:0.05; (e-f) 1:0.10

As previously stated, biochar is a material with a microporous structure that has a high surface area and good adsorption capacity. The addition of biochar to PCM will increase the area of functional groups which is beneficial for the absorption and dispersion of palmitic acid in biochar to prevent leakage phenomena during the phase change process. The functional group area of encapsulated PCM at different  $\text{TiO}_2$  additions can be seen in Figure 13 and Table 5. The more  $\text{TiO}_2$  is added, the functional group area is decreased. The reduction of the functional group area especially in the  $-\text{OH}$  and  $\text{C}=\text{O}$  groups explain the reduction of the weight loss of the palmitic acids means the small leakage phenomena still took place with the addition of  $\text{TiO}_2$  up to 20-25%.

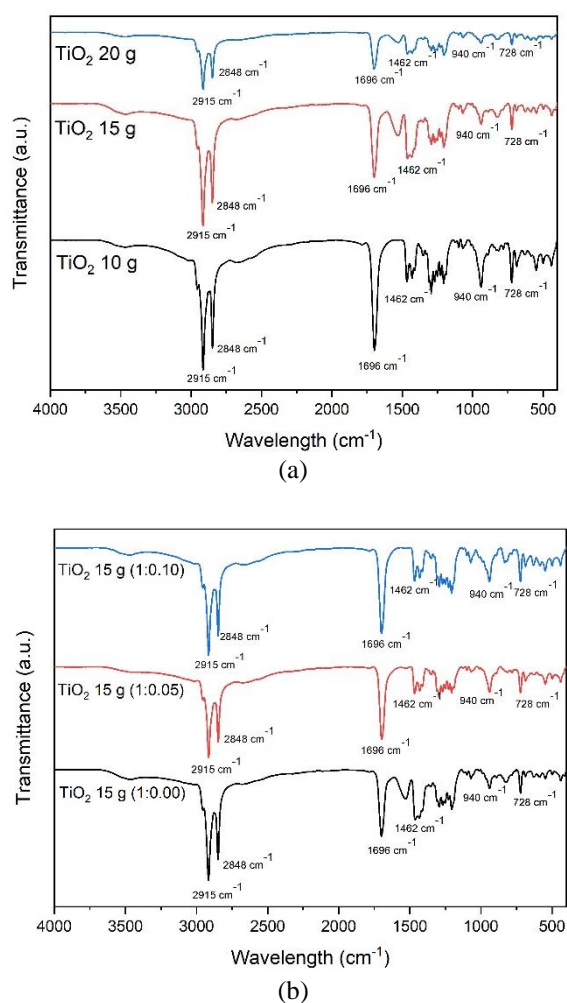


Figure 12. FTIR spectra of encapsulated PCM (a) at different  $\text{TiO}_2$  addition; (b) with 15 g  $\text{TiO}_2$  addition at variation of biochar ratio (w/w)

The addition of 15 gr  $\text{TiO}_2$  with variations of biochar ratio presented in Figure 14 and Table 6. The addition of biochar shows an increase in the functional

group area especially in the  $-\text{OH}$  and  $\text{C}=\text{O}$  groups. Common surface functional groups like  $\text{C}-\text{O}$ ,  $\text{C}=\text{O}$ , and  $-\text{OH}$  are normally existed in the pristine biochar (Huang et al., 2019; P. Zhang et al., 2022). The increment of the mentioned functional group led to the improvement of the anti-leakage properties as well as the thermal buffering properties as highlighted in the previous discussion.

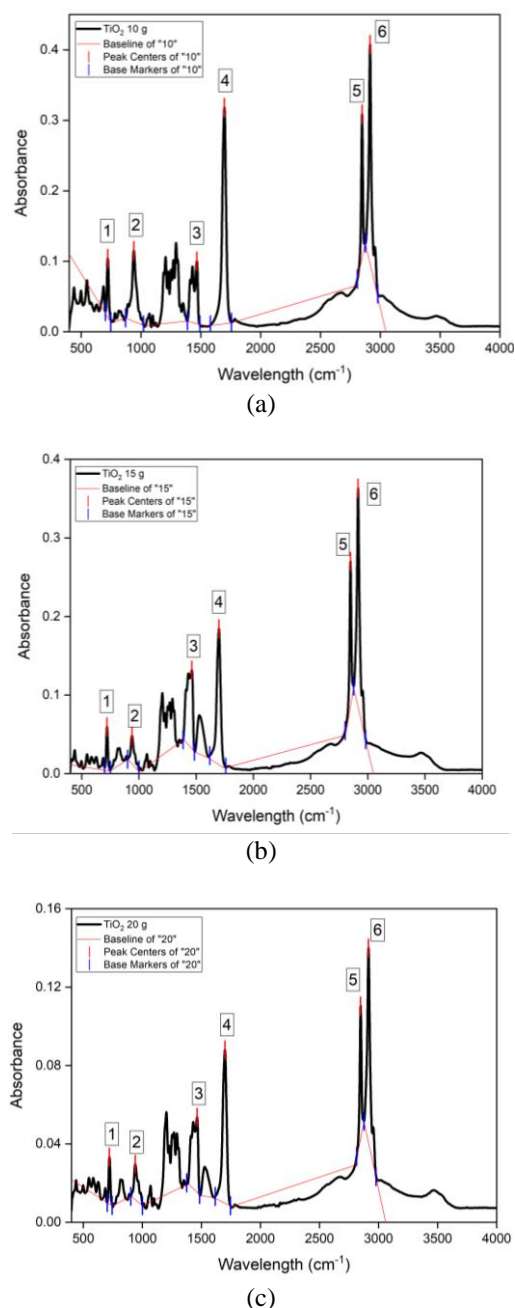


Figure 13. Functional group area of encapsulated PCM at different  $\text{TiO}_2$  addition (a) 10 g; (b) 15 g; (c) 20 gr

**Table 5.** Functional group area of encapsulated PCM at different TiO<sub>2</sub> addition

Peak No	Wavelength (cm <sup>-1</sup> )	Functional Group	Area		
			TiO <sub>2</sub> 10 g	TiO <sub>2</sub> 15 g	TiO <sub>2</sub> 20 g
1	728	Ti-O / -OH	1.53627	0.99995	0.4051
2	940	-OH	4.94346	1.37485	0.78283
3	1462	-CH <sub>3</sub> and -CH <sub>2</sub>	4.91949	6.22501	2.32517
4	1696	C=O	12.51937	7.27449	3.24195
5	2848	-CH <sub>3</sub> and -CH <sub>2</sub>	3.33931	3.60172	1.26889
6	2915	-CH <sub>3</sub> and -CH <sub>2</sub>	8.86252	8.64091	3.19392
<b>Total Area</b>			<b>36.12042</b>	<b>28.11693</b>	<b>11.21786</b>

**Table 6.** Functional group area of encapsulated PCM with 15 g TiO<sub>2</sub> addition at variation of biochar ratio (w/w)

Peak No	Wavelength (cm <sup>-1</sup> )	Functional Group	Area		
			TiO <sub>2</sub> 15 g (1:0.00)	TiO <sub>2</sub> 15 g (1:0.05)	TiO <sub>2</sub> 15 g (1:0.10)
1	728	Ti-O / -OH	0.99995	1.00765	1.26803
2	940	-OH	1.37485	2.79589	4.92162
3	1462	-CH <sub>3</sub> and -CH <sub>2</sub>	6.22501	3.66963	4.48714
4	1696	C=O	7.27449	8.88959	10.23672
5	2848	-CH <sub>3</sub> and -CH <sub>2</sub>	3.60172	2.44359	3.18922
6	2915	-CH <sub>3</sub> and -CH <sub>2</sub>	8.64091	6.16462	8.03638
<b>Total Area</b>			<b>28.11693</b>	<b>24.97097</b>	<b>32.13911</b>

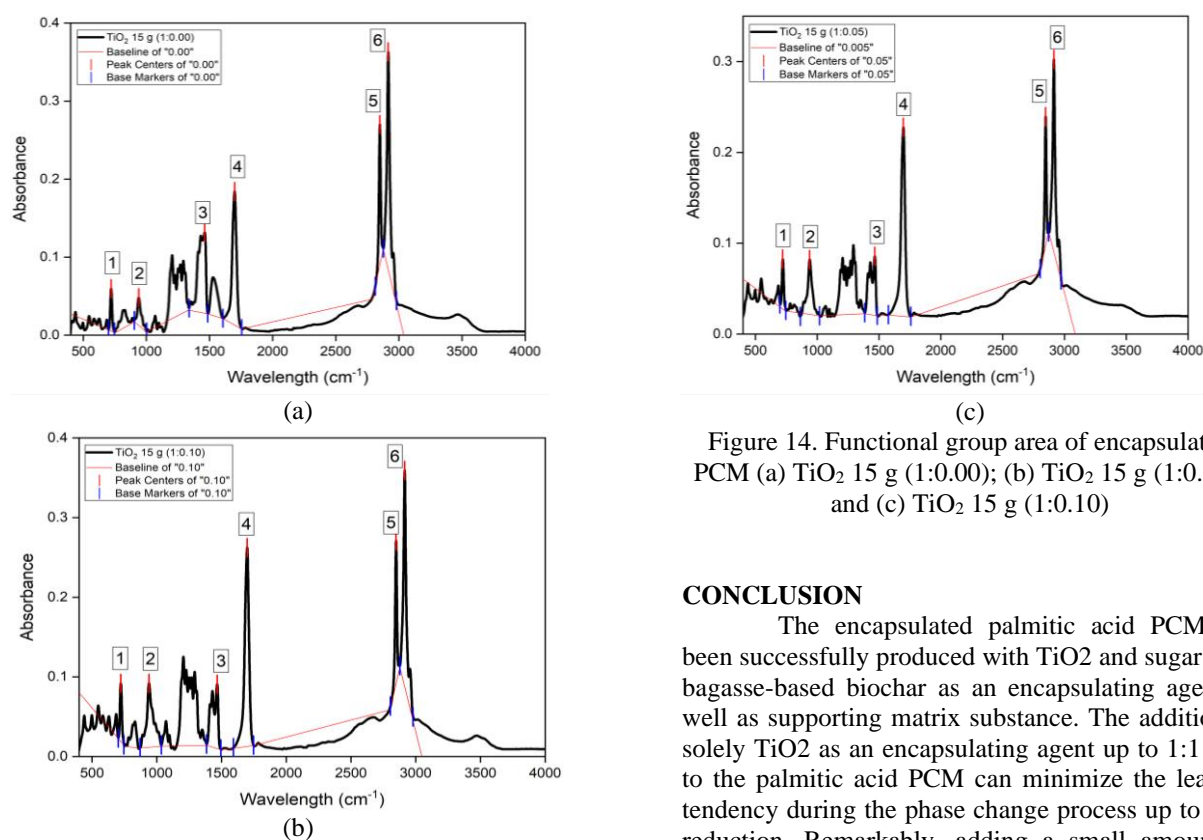


Figure 14. Functional group area of encapsulated PCM (a) TiO<sub>2</sub> 15 g (1:0.00); (b) TiO<sub>2</sub> 15 g (1:0.05); and (c) TiO<sub>2</sub> 15 g (1:0.10)

## CONCLUSION

The encapsulated palmitic acid PCM has been successfully produced with TiO<sub>2</sub> and sugar cane bagasse-based biochar as an encapsulating agent as well as supporting matrix substance. The addition of solely TiO<sub>2</sub> as an encapsulating agent up to 1:1 ratio to the palmitic acid PCM can minimize the leakage tendency during the phase change process up to 10% reduction. Remarkably, adding a small amount of supporting matrix substance (1: 0.1 w/w) sugar cane bagasse-based biochar into the encapsulating solution, has led to the production of a leak free palmitic acid PCM with enhanced thermal buffering properties. Small leakage detected with maximum 1.4% and

thermal buffering properties by keeping a package box temperature in the range of 2-8°C for more than 20 h by means small increment of temperature 0.72°C/h. The presence of biochar in the PCM-TiO<sub>2</sub> encapsulation system proposed to be reason of the improved properties of the palmitic acid PCM with additional surface functional group that absorbed PCM-TiO<sub>2</sub>.

## REFERENCES

- Alva, G., Huang, X., Liu, L., & Fang, G. (2017). Synthesis and characterization of microencapsulated myristic acid-palmitic acid eutectic mixture as phase change material for thermal energy storage. *Applied Energy*, 203.
- Ariyanti, D., Maillot, M., & Gao, W. (2018). Photo-assisted degradation of dyes in a binary system using TiO<sub>2</sub> under simulated solar radiation. *Journal of Environmental Chemical Engineering*, 6(1), pp. 539–548.
- Arofi, A. (2016). *Derajat Supercooling Serta Kinerja Larutan Eutektik Garam / H<sub>2</sub>O Untuk Cold Storage Berbasis Phase Change Material ( Pcm ) Derajat Supercooling Serta Kinerja Larutan Eutektik Garam / H<sub>2</sub>O Untuk Cold Storage Berbasis Phase Change*.
- Cao, L., Tang, F., & Fang, G. (2014). Preparation and characteristics of microencapsulated palmitic acid with TiO<sub>2</sub> shell as shape-stabilized thermal energy storage materials. *Solar Energy Materials and Solar Cells*, 123, pp.183–188.
- Drissi, S., Ling, T. C., & Mo, K. H. (2020). Development of leak-free phase change material aggregates. *Construction and Building Materials*, 230, pp.117029.
- Feng, L., Zheng, J., Yang, H., Guo, Y., Li, W., & Li, X. (2011). Preparation and characterization of polyethylene glycol/active carbon composites as shape-stabilized phase change materials. *Solar Energy Materials and Solar Cells*, 95(2), pp. 644–650.
- Harikrishnan, S., Imran Hussain, S., Devaraju, A., Sivasamy, P., & Kalaiselvam, S. (2017). Improved performance of a newly prepared nano-enhanced phase change material for solar energy storage. *Journal of Mechanical Science and Technology*.
- Huang, Q., Song, S., Chen, Z., Hu, B., Chen, J., & Wang, X. (2019). Biochar-based materials and their applications in removal of organic contaminants from wastewater: state-of-the-art review. *Biochar*, 1(1), pp.45–73.
- Li, C., He, G., Yan, H., Yu, H., & Song, Y. (2018). Synthesis of microencapsulated stearic acid with amorphous TiO<sub>2</sub> as shape-stabilized PCMs for thermal energy storage. *Energy Procedia*, 152, pp.390–394.
- Li, H., Chen, H., Li, X., & Sanjayan, J. G. (2014). Development of thermal energy storage composites and prevention of PCM leakage. *Applied Energy*, 135, pp.225–233.
- Li, L., Zhang, K., Chen, L., Huang, Z., Liu, G., Li, M., & Wen, Y. (2017). Mass preparation of micro/nanopowders of biochar with water-dispersibility and their potential application. *New Journal of Chemistry*, 41(18), pp.9649–9657.
- Liu, H., Wang, X., & Wu, D. (2017). Fabrication of Graphene/TiO<sub>2</sub>/Paraffin Composite Phase Change Materials for Enhancement of Solar Energy Efficiency in Photocatalysis and Latent Heat Storage. *ACS Sustainable Chemistry and Engineering*, 5(6), pp.4906–4915.
- Parameshwaran, R., Jayavel, R., & Kalaiselvam, S. (2013). Study on thermal properties of organic ester phase-change material embedded with silver nanoparticles. *Journal of Thermal Analysis and Calorimetry*, 114(2), pp.845–858.
- Ramakrishnan, S., Wang, X., Sanjayan, J., & Wilson, J. (2017). Assessing the feasibility of integrating form-stable phase change material composites with cementitious composites and prevention of PCM leakage. *Materials Letters*, 192, pp. 88–91.
- Sharma, R. K., Ganesan, P., Tyagi, V. v., Metselaar, H. S. C., & Sandaran, S. C. (2016a). Thermal properties and heat storage analysis of palmitic acid-TiO<sub>2</sub> composite as nano-enhanced organic phase change material (NEOPCM). *Applied Thermal Engineering*, 99, pp.1254–1262.
- Sharma, R. K., Ganesan, P., Tyagi, V. V., Metselaar, H. S. C., & Sandaran, S. C. (2016b). Thermal properties and heat storage analysis of palmitic acid-TiO<sub>2</sub> composite as nano-enhanced organic phase change material (NEOPCM). *Applied Thermal Engineering*, 99, pp.1254–1262.
- Singh, S. P., Burgess, G., & Singh, J. (2008). Performance comparison of thermal insulated packaging boxes, bags and refrigerants for single-parcel shipments. *Packaging Technology and Science*, 21(1), pp.25–35.
- Tao, Y. B., & He, Y. L. (2018). A review of phase change material and performance enhancement method for latent heat storage system. In *Renewable and Sustainable Energy Reviews* (Vol. 93, pp. 245–259). Elsevier Ltd.
- Wan, Y. chao, Chen, Y., Cui, Z. xing, Ding, H., Gao, S. feng, Han, Z., & Gao, J. kai. (2019a). A promising

form-stable phase change material prepared using cost effective pinecone biochar as the matrix of palmitic acid for thermal energy storage. *Scientific Reports*, 9(1), pp.1–10.

Wan, Y. chao, Chen, Y., Cui, Z. xing, Ding, H., Gao, S. feng, Han, Z., & Gao, J. kai. (2019b). A promising form-stable phase change material prepared using cost effective pinecone biochar as the matrix of palmitic acid for thermal energy storage. *Scientific Reports*, 9(1).

Wan, Y. chao, Chen, Y., Cui, Z. xing, Ding, H., Gao, S. feng, Han, Z., & Gao, J. kai. (2019c). A promising form-stable phase change material prepared using cost effective pinecone biochar as the matrix of palmitic acid for thermal energy storage. *Scientific Reports*, 9(1), pp.1–10.

Yang, Yim, Y.-J., Lee, K., Heo, & Park, Y.-S. (2019). Carbon-Filled Organic Phase-Change Materials for Thermal Energy Storage: A Review. *Molecules*, 24, 2055.

Zhang, P., Duan, W., Peng, H., Pan, B., & Xing, B. (2022). Functional Biochar and Its Balanced Design. *ACS Environmental Au*, 2(2), pp.115–127.

Zhang, X., Wang, X., & Wu, D. (2016). Design and synthesis of multifunctional microencapsulated phase change materials with silver/silica double-layered shell for thermal energy storage, electrical conduction and antimicrobial effectiveness. *Energy*, 111, pp.498–512.

Zhou, D., Zhou, Y., Yuan, J., & Liu, Y. (2020). Palmitic Acid-Stearic Acid/Expanded Graphite as Form-Stable Composite Phase-Change Material for Latent Heat Thermal Energy Storage. *Journal of Nanomaterials*, 2020.

Zhu, Y., Qin, Y., Wei, C., Liang, S., Luo, X., Wang, J., & Zhang, L. (2018). Nanoencapsulated phase change materials with polymer-SiO<sub>2</sub> hybrid shell materials: Compositions, morphologies, and properties. *Energy Conversion and Management*, 164(February), pp.83–92.